Ab initio study of low-dimensional quantum spin systems Sr_3NiPtO_6, Sr_3CuPtO_6, and Sr_3NiIrO_6

Soumyajit Sarkar, Sudipta Kanungo, and T. Saha-Dasgupta
S. N. Bose National Centre for Basic Sciences, Kolkata, India

(Received 10 August 2010; revised manuscript received 25 October 2010; published 15 December 2010)

Using first-principles density-functional theory, we investigate the electronic structure of a class of low-dimensional quantum spin systems of general formula $A_3BB'O_6$, which has drawn recent interest due to their intriguing magnetic properties. In our study, we focus on three compounds, Sr_3NiPtO_6, Sr_3CuPtO_6, and Sr_3NiIrO_6, formed from choices of $3d$ and $5d$ elements in B and B' sites. Based on our first-principles calculations, we derive the magnetic interactions and the single-ion anisotropies, which define the underlying spin models for the three compounds. Our study forms the basis for future investigations.

DOI: 10.1103/PhysRevB.82.235122 PACS number(s): 71.20.Be, 75.30.Et, 75.30.Gw

I. INTRODUCTION

Compounds having effective dimensionality lower than three dimensions have been of interest for long time to chemists and physicists because of their unconventional properties. The effective low dimensionality arises due to the interplay between the geometry and directional nature of the chemical bonding. This can give rise to highly anisotropic electronic interactions. Magnetic systems of low dimensionality where the anisotropic electronic interaction translates into anisotropic magnetic interaction are of particular interest. Such systems with small spins such as $S=\frac{1}{2}$ or $S=1$, are of further interest due to the additional feature of quantum nature of the spins. This can give rise to fascinating phenomenon such as formation of spin-gap states, spincharge separation, quantum criticality, etc.[1] A question of great relevance in this connection is that given such a compound what will be the underlying magnetic model. Magnetic susceptibility data are often fitted with assumed magnetic models. This procedure may give rise to nonunique answers due to rather insensitive nature of the magnetic susceptibility on the detail of the magnetic models. Microscopic understanding is therefore required for the sake of uniqueness.

In this study, we take up compounds with general formula $A_3BB'O_6$, where A is an alkaline earth Sr/Ca, and B and B' are transition-metal elements. These compounds form K_4CdCl_6-type structures consisting of $(BB'O_6)^{-6}$ chains formed by alternating face sharing BO_6 trigonal prism and $B'O_6$ octahedra. The chains are separated from each other by the intervening A^{+2} cations and form a hexagonal arrangement while viewed along the chain direction as shown in Fig. 1. The available literature on this family of compounds is vast due to various possible choices of B and B' ions, both of magnetic and nonmagnetic nature. A very well-studied compound[2] in this family is $Ca_3Co_2O_6$, where B and B' both are occupied by Co ions, one in low-spin state and another in high-spin state. This compound has recently received much attention due to its unusual and complicated magnetic phases.[3–5] Co based compounds like Ca_3CoRhO_6,[4,6,7] Ca_3CoMnO_6,[8,9] have been further studied in the context of spin-orbit interaction and possibility of multiferroic behavior. A number of compounds other than the above-mentioned compounds have been synthesized which show variety of interesting properties. See Ref. 10 for some representative references. For a review on the list of synthesized compounds, see Ref. 11.

In the present study, we focus on three such compounds, namely, Sr_3NiPtO_6, Sr_3CuPtO_6, and Sr_3NiIrO_6. In the first two compounds, the octahedral B' sites are occupied by $5d$ element Pt while the trigonal prism sites are occupied by two neighboring $3d$ elements in the periodic table, Ni and Cu in the two cases. For the first and third compounds, the trigonal prismatic sites are occupied by same element, namely, Ni while the octahedral B' sites are occupied by two neighboring $5d$ elements in the periodic table, Pt and Ir in the two cases. This provides a nice possibility to have a comparative study between different compounds within this interesting family whose components differ in their electronic configuration in terms of addition or subtraction of one electron. Experimentally, Sr_3NiPtO_6 was reported to show no evidence of long-range magnetic ordering down to a temperature[12,13] of 1.8 K along with large single-ion anisotropy while Sr_3CuPtO_6 was reported to exhibit $S=1/2$ Heisenberg chain-like behavior with substantially large interchain coupling[12] and possible existence of a gap in the spin excitation spectra.[14] Sr_3NiIrO_6, on the other hand, was reported to show ordering in disordered antiferromagnetic state[15] with signatures of significant ferromagnetic interactions.[16]

We have carried out density-functional-theory- (DFT-) based structural optimization and electronic-structure calculations of the three compounds, followed by their analysis in terms of construction of effective Wannier functions and the low-energy model Hamiltonians, and the calculation of magnetic exchange interactions. We have also carried out calculations in presence of spin-orbit coupling (SOC) to know its importance in three compounds which also provides us with the information of magnetic anisotropic energy. We considered three different basis sets, namely: the muffin-tin orbital- (MTO-) based linear muffin-tin orbital (LMTO) (Refs. 17 and 18) and Nth-order MTO (NMTO) (Ref. 19) method as implemented in the Stuttgart code, the plane-wave basis as implemented in the Vienna ab initio simulation package (VASP) (Refs. 20 and 21) and the linear augmented plane wave (LAPW) method as implemented in the WIEN2K (Ref. 22) code. The reliability of the calculations in the three basis sets have been cross checked. The electronic structure of Sr_3NiPtO_6 (Ref. 23) as well as Sr_3NiIrO_6 (Ref. 24) compounds have been recently calculated while to best of our knowledge the electronic structure of Sr_3CuPtO_6 has not

 ©2010 The American Physical Society

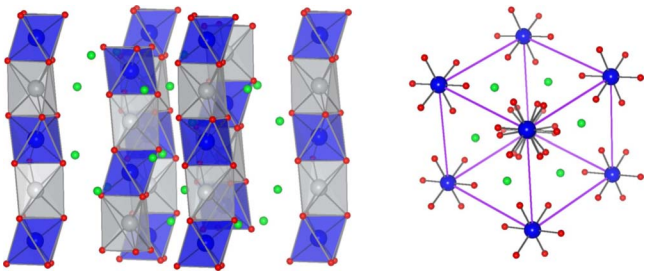

FIG. 1. (Color online) Left panel: crystal structure of $A_3BB'O_6$ compounds, showing the chains running along the vertical direction. Right panel: hexagonal packing of chains viewed along the chain direction. The blue (dark gray) and gray (light gray) colored balls denote B' and B atoms while red colored, small (dark gray, small) balls denote the shared oxygen atoms. A atoms, sitting in the hollows in between the chains are indicated with green (light gray), small balls.

been calculated. Our study in addition to calculation of electronic structures, as mentioned above, provides its analysis in terms of calculation of effective hopping interactions in the constructed Wannier basis, calculation of magnetic exchange interactions, and *ab initio* estimates of magnetic anisotropy energy. We also report the crystal structure data, considering theoretical optimization of the position of oxygen atoms, which may be useful for further study.

II. CRYSTAL STRUCTURE

Both Sr_3NiPtO_6 and Sr_3NiIrO_6 crystallize in rhombohedral crystal structure[12] with space group $R\bar{3}c$ consisting of perfectly linear Ni-B'-Ni (B'=Pt,Ir) chains with Ni-B'-Ni angle of 180°. The chains are arranged in a hexagonal arrangement as shown in the Fig. 1. Sr_3CuPtO_6 on the other hand shows distortion from this general structure. It consists of zigzag Cu-Pt-Cu chains with Cu-Pt-Cu angle deviating significantly from 180°, as shown in Fig. 2. This also ruins the perfect hexagonal arrangement of the chains in plane perpendicular to chain direction. The distortion causes lowering of the space-group symmetry from rhombohedral to monoclinic space group[12] of $C12/c1$. In view of the fact that the positions of light atoms are often not well characterized within the experimental technique, we have carried out the structural optimization of all three compounds relaxing the internal positions and keeping the lattice parameter fixed at the experimental values.[12,16,25] The optimizations were carried out using plane wave based pseudopotential framework of DFT as implemented in VASP.[20,21] The exchange correlation function was chosen to be that of generalized gradient approximation (GGA).[26] The position of the ions were relaxed toward equilibrium until the Hellmann-Feynman force becomes less than 0.01 eV/Å. $6\times6\times6$ k-point mesh and 500 eV plane-wave cutoff were used in these calculations. Table I shows the optimized coordinates.

The oxygen positions which are known for their relatively less sensitivity to x-ray are found to change in the theoretical optimization. The relaxed parameters associated with oxygen positions were found to change at most by 3%, compared to

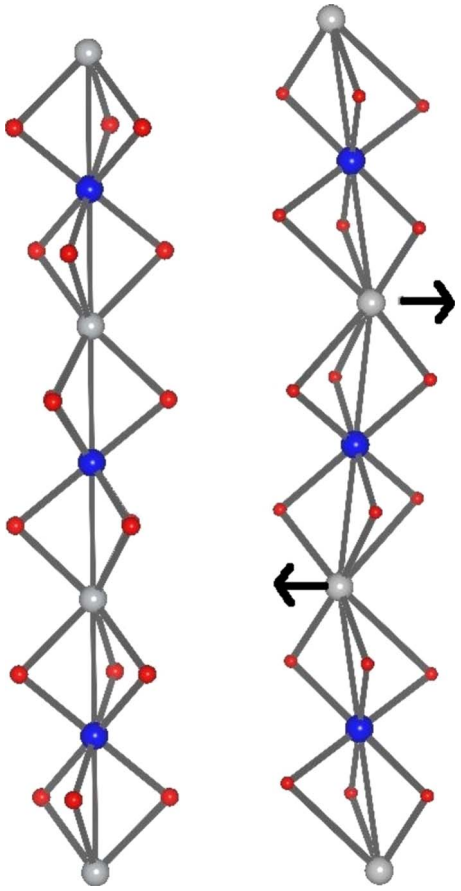

FIG. 2. (Color online) Comparison of $BB'O_6^{-6}$ chains in Sr_3NiPtO_6 and Sr_3NiIrO_6 compounds (left panel) and in Sr_3CuPtO_6 compound (right panel). The color convention is same as in Fig. 1.

experimentally measured parameters. The position of O3 atom for Sr_3CuPtO_6, particularly the z coordinate, however, was found to differ noticeably (a deviation of about 28%, see Ref. 25). Table II lists selected bond lengths and bond angle for the three compounds. For both Sr_3NiPtO_6 and Sr_3NiIrO_6 the trigonal prism is perfect with equal Ni-O bond lengths and O-Ni-O angles. The octahedra, though, shows the trigonal distortion with O-B'-O angles (B'=Pt,Ir) deviating from 90°. Both the trigonal prism as well as the octahedra are highly distorted in Sr_3CuPtO_6. In addition to trigonal distortion, the PtO_6 octahedra shows signature of small further distortion resulting into slightly different pairs of Pt-O bond lengths. The trigonal prism is also highly distorted with Cu atom not being at the center of the prism and O-O-O bond angles being different from 60°.

III. ELECTRONIC STRUCTURE

Figures 3 and 4 show the nonspin-polarized GGA density of states (DOS) and band structure for the three compounds, computed in LMTO basis.[17,18] Self-consistency was achieved through Brillouin-zone integrations over $8\times8\times8$ k points. The Sr-dominated states for all three compounds are empty, lying far away from the Fermi level (E_f) with very little contribution to states close to E_f, in conformity with the

TABLE I. Energy-minimized structural parameters of Sr_3NiPtO_6, Sr_3CuPtO_6, and Sr_3NiIrO_6. Lattice constants have been kept fixed at the experimental values (Refs. 12, 16, and 25).

Sr_3NiPtO_6						
a (Å)		c (Å)		x	y	z
9.583		11.196	Sr	0.364	0.0	0.25
			Ni	0.0	0.0	0.25
			Pt	0.0	0.0	0.0
			O	0.175	0.023	0.114
Sr_3CuPtO_6						
a (Å)	b (Å)	c (Å)	β (deg)	x	y	z
9.324	9.729	6.696	90.918	Sr1	0.314	0.073	0.622
				Sr2	0.0	0.105	0.25
				Cu	0.5	0.202	0.25
				Pt	0.25	0.25	0.0
				O1	0.213	0.314	0.714
				O2	0.356	0.428	0.073
				O3	0.055	0.339	0.050
Sr_3NiIrO_6						
a (Å)		c (Å)		x	y	z
9.586		11.132	Sr	0.364	0.0	0.25
			Ni	0.0	0.0	0.25
			Pt	0.0	0.0	0.0
			O	0.172	0.022	0.116

nominal Sr^{+2} valence. For Sr_3NiPtO_6 and Sr_3CuPtO_6 compounds, the states at E_f are Ni and Cu dominated, respectively, while for Sr_3NiIrO_6 the states at E_f are contributed by both Ni and Ir. In case of Sr_3NiPtO_6 and Sr_3CuPtO_6, Pt-dominated states are either completely full or completely empty. Ni d, Cu d and Ir d states show significant mixing with oxygen character. The band-structure plots show the m-decomposed contribution of d levels at B and B' sites, as well as O p and Sr-dominated characters. B' site being in octahedral environment, the d states are broadly split into B'-t_{2g} and B'-e_g while the splitting of d levels at B site is different due to trigonal prismatic environment of the surrounding oxygen atoms.[27] The orbital characters as marked in Fig. 4, are obtained in the local coordinate systems with local z axis pointing along the B' to apical O and the local y axis pointing approximately along the B'-in-plane O direction for the B' site. For the B site, the local z axis is chosen to point along the chain direction and the local y axis is chosen to point along approximately the in plane B-B direction. For Sr_3NiPtO_6, four half-filled bands cross E_f composing of Ni d_{yz} and Ni d_{xz} and contributed by two Ni atoms in the unit cell. The Pt t_{2g} levels appear below all the Ni d dominated states completely occupied while Pt e_g states remain empty with large crystal-field splittings of about 4 eV. For Sr_3CuPtO_6, on the other hand two bands cross E_f contributed by Cu d_{xz} character and two Cu atoms in the unit cell. Pt Pt t_{2g}-dominated bands unlike Sr_3NiPtO_6 compound appear in between the crystal-field split levels of Cu d with Pt e_g states being empty and with a t_{2g}-e_g crystal-field splitting of about 4 eV. For Sr_3NiIrO_6 six bands cross E_f, four contributed by Ni d_{yz} and Ni d_{xz} character and two contributed by Ir t_{2g} character. The rest of the Ir t_{2g} dominated bands appear in between the crystal field split Ni d levels. Ir t_{2g}-e_g splitting turn out to about 4 eV. Note that in absence of the spin ordering, the electronic structure of all three compounds suggest metallic character, which is due to insufficient treatment of electron-electron correlation in the GGA approximation. Interestingly, the spin-polarized calculations within GGA, drives the insulating solution since the energy-level positioning of various ions are such that states are either completely empty or filled in one specific spin channel (see Fig. 5 and discussions following this in the subsequent section).

While the magnetic ordering in these compounds are debated[13,14,28] and sometimes there exist clear indication of lack of ordering,[13] the spin-polarized electronic-structure calculations are helpful to decide on the spin state of the component ions. Table III shows the calculated magnetic mo-

TABLE II. Selected bond lengths and bond angles for the optimized crystal structure of Sr_3NiPtO_6, Sr_3CuPtO_6, and Sr_3NiIrO_6.

	Sr_3NiPtO_6	Sr_3CuPtO_6	Sr_3NiIrO_6
		$B'O_6$ octahedron	
∠O-B'-O (deg)	84.52, 95.34	80.63, 99.36	84.65, 95.34
	84.52, 95.34	87.69, 92.30	84.65, 95.34
	84.52, 95.34	87.11, 92.88	84.65, 95.34
B'-O distance (Å)	2.02	2.03,2.02,2.04	2.00
O-O distance (Å)	2.72, 3.00	2.93, 2.81	2.70, 2.96
		2.94, 3.09	
		2.80, 2.62	
		BO_6 trigonal prism	
∠O-O-O (deg)	60.0	62.48, 61.83	60.0
		55.68	
B-O distance (Å)	2.19	2.80, 2.02, 1.99	2.18
O-O distance (Å)	2.72	2.80,2.81,2.62	2.70
	3.06	3.52, 3.50, 3.50	3.06
		B-B' chain	
∠B'-B-B' (deg)	180	161.37	180

ments at B, B', and O sites, as obtained in spin-polarized GGA calculations. We find both Pt^{4+} with d^6 configuration and Ir^{+4} ion with d^5 configuration are in low-spin states, giving rise to $S=0$ and $S=1/2$ spin states, respectively. The magnetic moments at Ni^{2+} with d^8 configuration and Cu^{2+} with d^9 configuration suggest $S=1$ and $S=1/2$ spin states respectively. Non-negligible moments at oxygen sites indicate substantial hybridization between oxygen and Ni or Cu or Ir degrees of freedom, as has been pointed out already. These results indicate 1–0-1–0-1–0 type of spin chain structure in case of Sr_3NiPtO_6 compound, $\frac{1}{2}$-0-$\frac{1}{2}$-0-$\frac{1}{2}$-0-type spin chain structure in case of Sr_3CuPtO_6 compound and 1-$\frac{1}{2}$-1-$\frac{1}{2}$-1-$\frac{1}{2}$-type spin chain structure in case of Sr_3NiIrO_6 compound. Sr_3NiPtO_6 and Sr_3CuPtO_6 compounds therefore represent the case with B being occupied by the magnetic ion, B' being nonmagnetic while Sr_3NiIrO_6 gives rise to situation where both B and B' are magnetic.

IV. LOW-ENERGY HAMILTONIANS AND HOPPING INTERACTIONS

In Fig. 5 we present the energy-level diagram and their occupancies for B and B' sites as given by DFT for the three compounds. Due to the presence of finite distortion, the levels are not of pure character but are of mixed character. What is indicated for each level is the dominated character. Due to presence of trigonal distortion in $B'O_6$ octahedra for Sr_3NiPtO_6 and Sr_3NiIrO_6 compounds, the t_{2g}'s get mixed and one should ideally use e_g^π and a_{1g} symmetries with doubly degenerate e_g^π's and singly degenerate a_{1g}. We prefer to designate them as $t_{2g}^{(1)}$, $t_{2g}^{(2)}$, and $t_{2g}^{(3)}$, and the similarly, $e_g^{(1)}$ and $e_g^{(2)}$, for the e_g^σ levels. In case of Sr_3CuPtO_6 compound, due

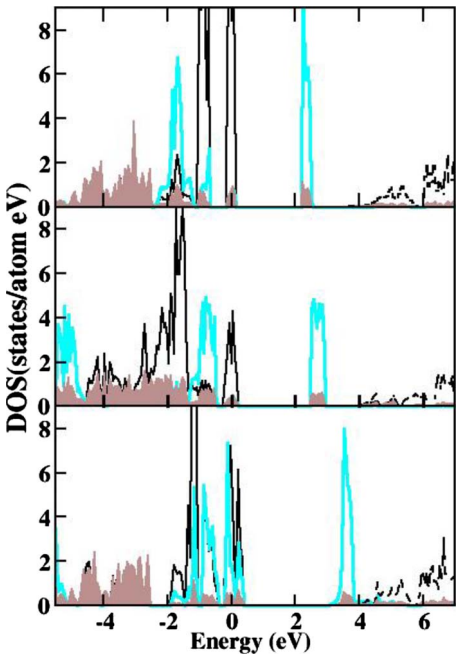

FIG. 3. (Color online) Nonspin-polarized DOS calculated within GGA. B'-d states, B-d states, Sr s, and O p states are presented by solid black lines (black in color), gray lines (cyan in color), broken black lines (black in color), and filled gray lines (brown in color), respectively. The zero of the energy is set at E_f. From top to bottom, the three panels correspond to plots for Sr_3NiPtO_6, Sr_3CuPtO_6, and Sr_3NiIrO_6 compounds, respectively.

to additional distortion, the degeneracies get completely lifted. The spin models for the Sr_3NiPtO_6, Sr_3CuPtO_6, and Sr_3NiIrO_6 compounds therefore can be constituted in terms of Ni d_{yz} and d_{xz} degrees of freedom, Cu d_{xz} degree of freedom, and Ni d_{yz} and Ni d_{xz} degrees of freedom combined with Ir $t_{2g}^{(3)}$ degrees of freedom, respectively.[29] For this purpose we carried out NMTO-downfolding calculation starting from full DFT calculations. NMTO-downfolding calculation is an energy selective procedure that produces the low en-

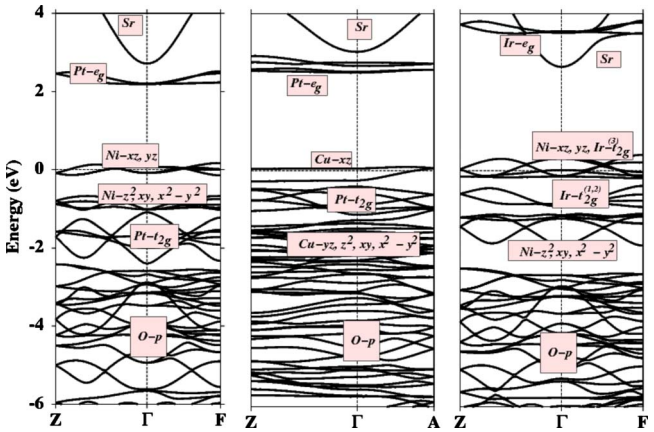

FIG. 4. (Color online) Nonspin-polarized band-structure calculated within GGA. The dominant orbital characters for the bands are indicated. Zero of the energy is set at E_f. From left to right, the three panels correspond to plots for Sr_3NiPtO_6, Sr_3CuPtO_6, and Sr_3NiIrO_6, respectively.

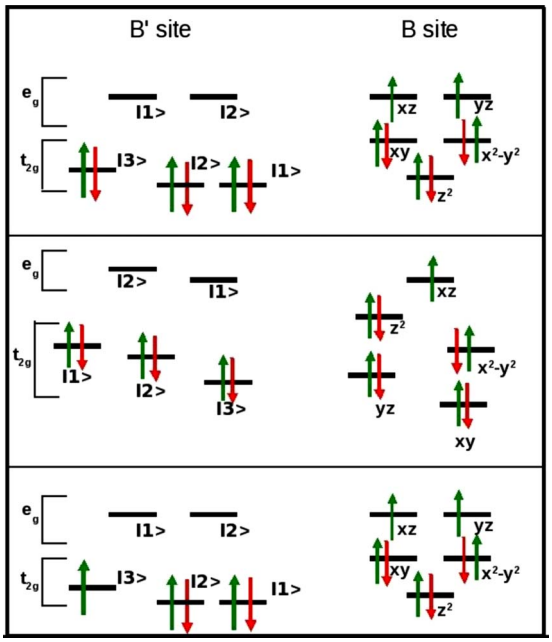

FIG. 5. (Color online) The energy levels of B-d and B'-d levels in eV unit and their occupancies. From top to bottom, the three panels correspond to plots for Sr_3NiPtO_6, Sr_3CuPtO_6, and Sr_3NiIrO_6, respectively.

ergy, few orbital Hamiltonian defined in the effective Wannier function basis by integrating out the degrees of freedom that are not of interest. For our downfolding calculations, therefore, we have kept only Ni d_{yz} and Ni d_{xz} degrees of freedom active in case of Sr_3NiPtO_6, Cu d_{xz} degrees of freedom active in case of Sr_3CuPtO_6 and Ni d_{yz}, and Ni d_{xz} and Ir $t_{2g}^{(3)}$ degrees of freedom active in case of Sr_3NiIrO_6 compound and downfolded all other degrees of freedom. These give rise to low-energy Hamiltonians of dimensions 4×4, 2×2, and 6×6 in three cases. Diagonalization of these Hamiltonians at various k points produce the downfolded band structure which are in excellent agreement with full DFT band structure as shown in Fig. 6.

Fourier transforms of the downfolded, low-energy Hamiltonians provide us[19] with the information of effective Ni-Ni, effective Cu-Cu, and effective Ni-Ir, Ni-Ni, and Ir-Ir hopping interactions defined in a Wannier function basis for Sr_3NiPtO_6, Sr_3CuPtO_6, and Sr_3NiIrO_6 compounds, respectively. Table IV lists the dominant hopping interactions and Fig. 7 shows the corresponding hopping paths. The strongest hopping interaction turns out to be the intrachain interaction for all three compounds. Figure 8 shows the overlap of effective Wannier functions, defining the exchange paths for the intrachain interactions. While the central part of the Wannier functions are shaped according to Ni d_{xz}/d_{yz} or Cu d_{xz} or Ir $t_{2g}^{(3)}$ symmetry, the tails sitting at neighboring sites are shaped according to integrated out degrees of freedom such as O p or Pt d or other integrated out d symmetries at B and B'. In case of Sr_3NiPtO_6 and Sr_3CuPtO_6, as is seen from the overlap of two neighboring Ni d_{xz} or d_{yz} Wannier functions with each other and two Cu d_{xz} Wannier functions, respectively, the exchange paths are formed by Ni-O-O-Ni and Cu-O-O-Cu super-superexchanges, respectively. Small but nonzero weights are seen at intervening Pt sites too. For Sr_3NiIrO_6 compound, the exchange, as is seen from the path formed by overlap of Ni d_{xz}/d_{yz} Wannier functions with neighboring Ir $t_{2g}^{(3)}$ Wannier function, is mediated through connecting oxygen atoms as well as through direct overlap of Ni d_{xz}/d_{yz} with Ir $t_{2g}^{(3)}$, in the sense of presence of finite weights of the tails belonging to Ni(Ir) Wannier function at Ir(Ni) site. Examination of hopping interactions indicates also presence of rather large Ni-Ni interactions (t_5) mediated by both oxygen and Ir.

TABLE III. Magnetic moments at B, B', and O sites, as obtained in spin-polarized GGA calculations.

	Magnetic moment in μ_B		
	Sr_3NiPtO_6	Sr_3CuPtO_6	Sr_3NiIrO_6
B	1.43	0.50	1.34
B'	0.02	0.02	0.81
O	0.08	0.06	0.14

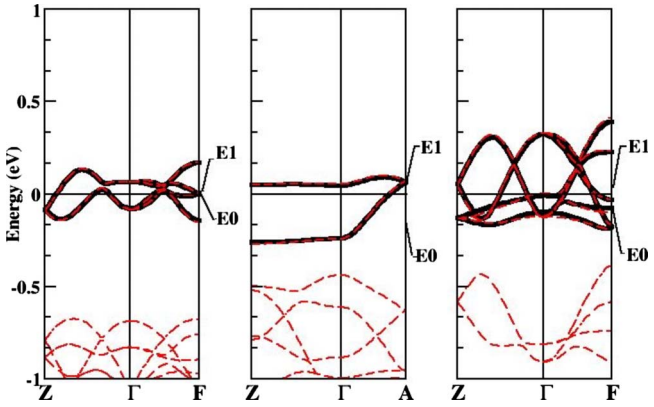

FIG. 6. (Color online) Bands obtained with downfolded basis (solid lines) compared to full DFT band structure (dashed lines). The energy points marked as E_0 and E_1 in each panel, denote the energy points used in NMTO calculation. From left to right, the three panels correspond to plots for Sr_3NiPtO_6, Sr_3CuPtO_6, and Sr_3NiIrO_6, respectively.

For the Sr_3NiPtO_6 and Sr_3NiIrO_6 compounds, the interchain hoppings turn out to be considerably smaller than the intrachain hoppings, while for Sr_3CuPtO_6 compound, the interchain interactions turn out to be significant fraction of the intrachain interaction. The fact that the interchain interactions are significant and that Sr_3CuPtO_6 should not be considered as magnetically one dimensional has been pointed out in past studies[12,14] using fitting of the susceptibility data.

V. MAGNETIC INTERACTION

Given the knowledge of hopping interactions, it is possible to calculate the magnetic interactions, employing the superexchange expressions. However, because of the complicated exchange paths such energies are not easy to estimate. We therefore attempted to estimate the magnetic interaction

TABLE IV. List of dominant hopping interactions for the three compounds. In case of Sr_3NiPtO_6, hoppings are defined between Ni d_{xz}/d_{yz} and Ni d_{xz}/d_{yz}. In case of Sr_3CuPtO_6, hoppings are defined between Cu d_{xz} and Cu d_{xz}. For Sr_3NiIrO_6, hoppings are defined between Ni d_{xz}/d_{yz} and Ir $t_{2g}^{(3)}$ as well as between Ni d_{xz}/d_{yz} and Ni d_{xz}/d_{yz}, and between Ir $t_{2g}^{(3)}$ and Ir $t_{2g}^{(3)}$.

Sr_3NiPtO_6					
Distance(Å)	(connecting vector)				
Hopping Int. (meV)					
5.60	(0 0 1)	(0 0 −1)	...	...	...
t_1 (Intra chain)	$\begin{pmatrix} 37.9 & 0.0 \\ 0.0 & 37.9 \end{pmatrix}$	$\begin{pmatrix} 37.9 & 0.0 \\ 0.0 & 37.9 \end{pmatrix}$			
6.67	(−1 0 −.68)	(1 0 .68)	...	...	...
t_2 (Inter chain)	$\begin{pmatrix} 15.4 & -8.9 \\ 8.9 & -2.7 \end{pmatrix}$	$\begin{pmatrix} 15.4 & 8.9 \\ -8.9 & -2.7 \end{pmatrix}$			
6.67	(.5 −.87 −.68)	(.5 .87 .68)	(−.5 −.87 .68)	(−.5 .87 .68)	...
t_3 (Inter chain)	$\begin{pmatrix} 1.8 & -1.1 \\ 16.7 & 10.8 \end{pmatrix}$	$\begin{pmatrix} 1.8 & -16.7 \\ 1.1 & 10.8 \end{pmatrix}$	$\begin{pmatrix} 1.8 & 1.1 \\ -16.7 & 10.8 \end{pmatrix}$	$\begin{pmatrix} 1.8 & 16.7 \\ -1.1 & 10.8 \end{pmatrix}$	

Sr_3CuPtO_6			Sr_3NiIrO_6		
Distance (Å)	(connecting vector)		Distance (Å)	(connecting vector)	
Hopping Int. (meV)			Hopping Int. (meV)		
5.77	(−.48 −.1 −.34)	(.48 −.1 .34)	2.78	(0 0 −.5)	(0 0 .5)
t_1 (Intra Chain)	68.5	68.5	t_1 (Intra chain)	$\begin{pmatrix} 39.8 \\ 56.9 \end{pmatrix}$	$\begin{pmatrix} 39.8 \\ -56.9 \end{pmatrix}$
6.69	(0 0 −.69)	(0 0 .69)	5.56	(0 0 1)	(0 0 −1)
t_2 (Inter chain)	31.1	-31.1	t_2 (Inter chain)	-18.0	-18.0
9.32	(0 0 −.69)	(0 0 .69)	5.83	(−.5 .87 −.34)	(−.5 −.87 −.34)
t_3 (Inter chain)	12.5	-12.5	t_3(Inter chain)	8.4	8.4
...	...	...	6.66	(.5 −.87 −.67)	(−.5 .87 .67)
			t_4(Inter chain)	13.8	13.8
...	...	...	5.56	(0 0 −1)	(0 0 1)
			t_5 (Intra chain)	$\begin{pmatrix} 92.9 & 5.9 \\ 5.9 & 85.3 \end{pmatrix}$	$\begin{pmatrix} 92.9 & -5.9 \\ -5.9 & 85.3 \end{pmatrix}$

using the total energy calculation of various spin configuration and mapping the DFT total energy to corresponding Ising Model.[30] Calculations have been carried out within the framework of plane wave basis in VASP within GGA. Though such a scheme is also faced with several difficulties such as the choice of spin configurations, choice of basis sets, and exchange-correlation functional, it is expected to provide us with indicative estimates. The total energy calculations show the strongest intrachain interaction, J, for Sr_3NiPtO_6 and Sr_3CuPtO_6 compounds to be of antiferromagnetic nature with values 1.12 meV and 2.25 meV, respectively, and of ferromagnetic nature for Sr_3NiIrO_6 compound. For Sr_3NiIrO_6 compound, we failed to stabilize any other magnetic configuration, other than ferromagnetic alignment of Ni and Ir spins along a chain. Any other chosen configuration, converged to ferromagnetic solution, proving the robustness of the ferromagnetic alignment of Ni and Ir spins over other solutions. In order to check the influence of correlation effect beyond GGA approach on the magnetic interactions, we have repeated the calculations within GGA+U framework[31] as well. The calculations were carried out for two choice of U values at B site (U=3.5 eV and U=5 eV), keeping U value at B' site to be fixed at 1.5 eV. The Hund's exchange J_H was chosen to be 0.8 eV. As expected, the values of the dominant intrachain magnetic exchanges, which are of antiferromagnetic nature for Sr_3NiPtO_6 and Sr_3CuPtO_6 compounds, were found to decrease with increasing U values with values 0.94 meV for U=3.5 eV and 0.61 meV for U=5 eV for Sr_3NiPtO_6, and 2.12 meV for U=3.5 eV, and 1.57 meV for U=5 eV for Sr_3CuPtO_6. For Sr_3NiIrO_6, even with application of U, we failed to stabilize any other configuration other than ferromagnetic arrangement between Ir and Ni spins.

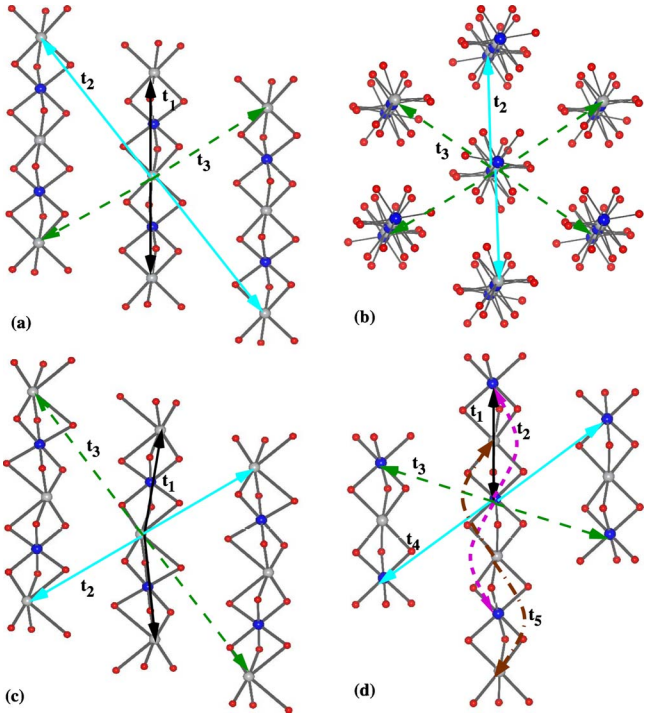

FIG. 7. (Color online) Panels (a) and (b): Ni-Ni hopping interaction paths, t_n in Sr_3NiPtO_6. Panels (a) and (b) show perspectives showing the chains and that viewed along the chain direction, showing the hexagonal packing. Panel (c): Cu-Cu interaction paths, t_n in Sr_3CuPtO_6. Panel (d): Ni-Ni, Ni-Ir, and Ir-Ir interaction paths, t_n in Sr_3NiIrO_6. The color convention of atoms is same as in Fig. 1.

The antiferromagnetic and ferromagnetic nature of intrachain interactions may be understood considering the energy level diagrams as shown in Fig. 5 and the exchange paths shown in Fig. 8. For Sr_3NiPtO_6 compound the intrachain Ni-Ni interaction occurs between half-filled Ni $d_{xz/yz}$ levels through the oxygen-mediated superexchange paths as shown in Fig. 8, which according Kugel-Khomskii-type picture[32] would give rise to antiferromagnetic interaction. Similarly the intrachain Cu-Cu interaction in case of Sr_3CuPtO_6 compound occurs between half-filled Cu d_{xz} levels through the superexchange path shown in Fig. 8, giving rise to antiferromagnetic interaction. For Sr_3NiIrO_6 compound, while the exchange occurring between half-filled Ni d_{xz}/d_{yz} and Ir $t_{2g}^{(3)}$ is of antiferromagnetic nature, there exist an additional exchange interaction between half-filled Ni d_{xz}/d_{yz} and empty Ir e_g^{σ} states which according to Kugel-Khomskii picture, would be ferromagnetic in nature. The later exchange, though, is expected to be weak due to large energy separation between Ni d_{xz}/d_{yz} and Ir e_g^{σ} levels. We, however, notice a direct exchange path between Ni d_{xz}/d_{yz} and Ir $t_{2g}^{(3)}$, as described previously, which would give rise to ferromagnetic contribution. Interestingly, intrachain Ni-Ni interaction (the magnetic interaction, corresponding to the hopping t_5) also turned out to be ferromagnetic, presumably due to substantial contribution through path involving Ir. Our obtained result of ferromagnetic intrachain interaction is in contradiction with that obtained in theoretical study of Ref. 24. The conclusions inferred from the experimental data, are debated with some supporting ferromagnetic intrachain interaction[16] and others proposing antiferromagnetic intrachain interaction.[15] Further experiments are necessary to resolve this controversy. The small interchain interaction in case of Sr_3NiPtO_6 compound turned out to be ferromagnetic nature with value 0.10 meV. The substantial interchain interaction (J') in the case of Sr_3CuPtO_6 compound turned out to be antiferromagnetic nature, with value 0.65 meV, giving rise to a ratio of $J/J' \approx 3.5$, in good agreement with the estimates obtained from the analysis of magnetic measurements.[12,14] The interchain interactions for Sr_3NiIrO_6, on the other hand, turned out to be antiferromagnetic, presumably explaining the signature of antiferromagnetic couplings observed in experiments.[15]

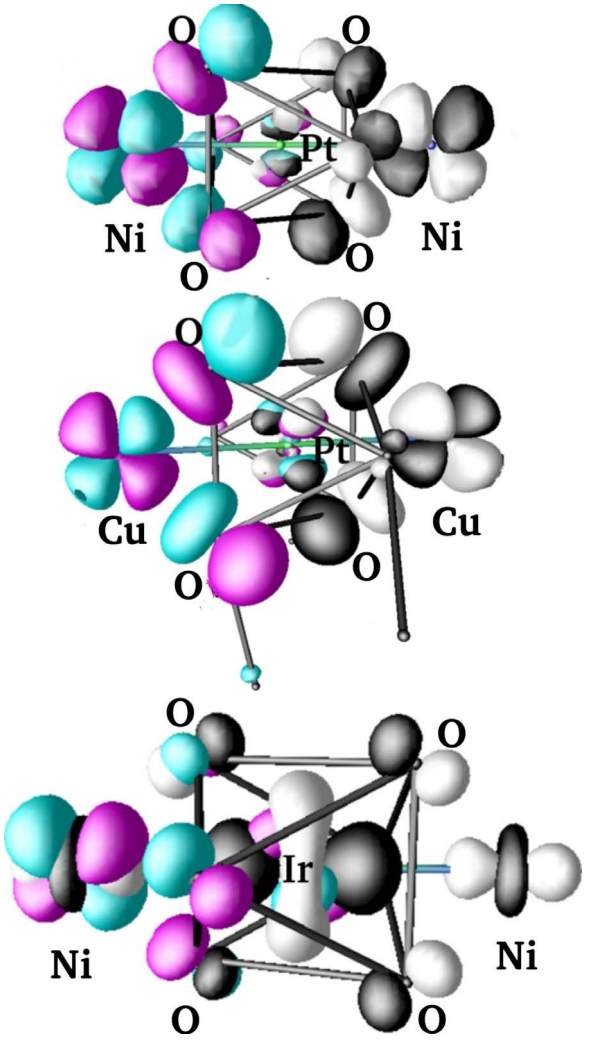

FIG. 8. (Color online) Effective orbitals corresponding to the downfolded d_{xz} NMTOs, placed at two Ni (Sr_3NiPtO_6, top panel) or two Cu (Sr_3CuPtO_6, middle panel) situated in a given chain. For Sr_3NiPtO_6 an equivalent superexchange path exists, created by overlap of two Ni downfolded d_{yz} NMTOs. The bottom panels show the overlap of downfolded Ni d_{xz} and Ir $t_{2g}^{(3)}$ NMTOs placed at neighboring sites within a chain. Other intrachain superexchange paths involve overlap of Ni d_{yz} with Ir $t_{2g}^{(3)}$ and Ni d_{xz}/d_{yz} with Ni d_{xz}/d_{yz}. Lobes of orbitals placed at different sites are colored differently. Lobe colored black (white) at one site represents the same sign as that colored magenta (cyan) at other neighboring site.

TABLE V. Spin and orbital moments in μ_B as obtained in GGA+SO calculations for the three compounds (Ref. 33). The magnetic anisotropy energies are also listed.

		Sr_3NiPtO_6		Sr_3CuPtO_6		Sr_3NiIrO_6	
		Direction with respect to B-B' chain					
Spin-quantization axis		$\parallel$	$\perp$	$\parallel$	$\perp$	$\parallel$	$\perp$
Orbital moment	B	0.22	0.16	0.13	0.13	0.21	0.27
	B'	0.0	0.0	0.0	0.0	−0.01	−0.11
Spin moment	B	1.46	1.46	0.53	0.50	1.39	1.46
	B'	0.02	0.02	0.02	0.03	0.41	0.42
Anisotropy energy $E=E_{\parallel}-E_{\perp}$		−0.75 meV		−0.12 meV		13.5 meV	

VI. SPIN-ORBIT INTERACTION

The importance of spin-orbit interaction and single-ion anisotropy in these compounds has been discussed in literature.[12,28] In order to investigate that we carried out calculations within the framework of GGA+SO. The calculations have been carried out using the LAPW basis as implemented within WIEN2K code.[22] The number of plane waves were restricted using the criteria muffin-tin radius multiplied k_{max} yielding a value of 7. The spin-quantization axis was chosen to be parallel to the direction of the chain as well as perpendicular to the chain direction. Table V lists spin and orbital moments at B and B' sites, as obtained within GGA +SO calculations. We find rather large orbital moments at Ni and Cu sites, pointing parallel to the spin moment due to more than half-filled nature of Ni d or Cu d occupancies. The orbital moment at Pt site is negligibly small due to the completely filled t_{2g} occupancies while that of Ir site is large which point opposite to the spin moment. The substantial orbital moment at Ni site is unexpected due to its d^8 configuration and the trigonal prismatic environment driven splitting of energy levels which results into complete quenching of the orbital degree of freedom. The presence of finite and substantially large orbital moment at Ni site[34] therefore needs to be justified as an induced mechanism due to the mixing of the ligand, namely, O p orbitals. Similar situation is expected to occur for Cu which is in d^9 state with quenched orbital degrees of freedom. The magnetocrystalline anisotropy obtained by taking the energy difference between calculations with spin quantization chosen along the chain direction and perpendicular to the chain direction yields values 0.75 meV per Ni ion for Sr_3NiPtO_6, 0.12 meV per Cu ion for Sr_3CuPtO_6, and 13.5 meV per formula unit for the Sr_3NiIrO_6 compound. In case of Sr_3NiPtO_6 and Sr_3CuPtO_6 compounds, the spin quantization is found to be favored along the chain direction, giving rise to an easy axis scenario while for Sr_3NiIrO_6 compound the spin quantization favors lying in the plane perpendicular to the chain direction giving rise to easy-plane scenario. The magnetocrystalline anisotropy is large for Sr_3NiIrO_6 compound with both Ni and Ir contributing, comparatively smaller for Sr_3NiPtO_6 and a tiny one for Sr_3CuPtO_6 compound. In order to check the influence of missing correlation effect in magnetocrystalline anisotropy energy, like in case of magnetic interactions, we have repeated the calculations within the framework of GGA+U+SO. While the quantitative values were found to decrease upon application of U, the trend was found to remain intact. The experimental study carried out for Sr_3NiPtO_6 predicted[12] the easy plane scenario on the basis of susceptibility measurement and fit carried out with an assumed model. Our obtained parameters for Sr_3NiPtO_6, therefore will be important to resolve whether the experimental results should be interpreted in terms of a nontrivial spin-liquid state of an easy axis magnet or a simple easy-plane single-ion effect.

VII. CONCLUSION

To conclude, using first-principles DFT calculations, we have investigated the electronic structure of three compounds, Sr_3NiPtO_6, Sr_3CuPtO_6, and Sr_3NiIrO_6, belonging to the class of low-dimensional quantum spin systems of general formula, $A_3BB'O_6$. Analyzing the results of electronic-structure calculations in terms of formation of low-energy Hamiltonians defined in the basis of effective Wannier functions and calculation of magnetic interactions in terms of total energy calculations, we derived the underlying spin model for each of these compounds. The magnetocrystalline anisotropy energies were evaluated from calculations in presence of SOC. The intrachain interactions are found to be the dominant interactions in all three cases, which turned out to be of antiferromagnetic nature for Sr_3NiPtO_6 and Sr_3CuPtO_6 compounds, and to be of ferromagnetic nature for Sr_3NiIrO_6 compound. The interchain interactions are found to be small and of ferromagnetic nature for Sr_3NiPtO_6 compound, substantially large and of antiferromagnetic nature for Sr_3CuPtO_6 compound, and of antiferromagnetic nature for Sr_3NiIrO_6 compound. Large anisotropy is found for Sr_3NiIrO_6 compound with appreciable value for Sr_3NiPtO_6 compound and a small value for Sr_3CuPtO_6 compound. The magnetic anisotropy is found to be of easy axis in case of Sr_3NiPtO_6 and Sr_3CuPtO_6 compounds while it is found to be of easy plane for Sr_3NiIrO_6 compound. While some of our results are in agreement with existing experimental observations, some are not.[12,14–16] Our detail investigation, therefore, form the basis for further experimental investigations. It also

provides the basis of further theoretical studies in terms of solution of the proposed spin models which can give rise to variety of properties in the parameter space of intrachain and interchain interactions as well as easy axis versus easy-plane situations.

ACKNOWLEDGMENTS

The authors gratefully acknowledge discussions with K. Damle and for bringing these compounds into notice. S.S. thanks CSIR for financial support.

[1] P. Lemmens, G. Guntherodt, and C. Gros, Phys. Rep. **375**, 1 (2003).
[2] H. Wu, M. W. Haverkort, Z. Hu, D. I. Khomskii, and L. H. Tjeng, Phys. Rev. Lett. **95**, 186401 (2005).
[3] J. An and C.-W. Nan, Solid State Commun. **129**, 51 (2004).
[4] M.-H. Whangbo, D. Dai, H.-J. Koo, and S. Jobic, Solid State Commun. **125**, 413 (2003).
[5] R. Fresard, C. Laschinger, T. Kopp, and V. Eyert, Phys. Rev. B **69**, 140405(R) (2004).
[6] H. Wu, Z. Hu, D. I. Khomskii, and L. H. Tjeng, Phys. Rev. B **75**, 245118 (2007).
[7] E. V. Sampathkumaran and A. Niazi, Phys. Rev. B **65**, 180401(R) (2002).
[8] H. Wu, T. Burnus, Z. Hu, C. Martin, A. Maignan, J. C. Cezar, A. Tanaka, N. B. Brookes, D. I. Khomskii, and L. H. Tjeng, Phys. Rev. Lett. **102**, 026404 (2009).
[9] Y. J. Choi, H. T. Yi, S. Lee, Q. Huang, V. Kiryukhin, and S.-W. Cheong, Phys. Rev. Lett. **100**, 047601 (2008).
[10] C. Lampe-Onnerud, M. Sigrist, and H. Loye, J. Solid State Chem. **127**, 25 (1996); S. Rayaprol, K. Sengupta, E. V. Sampathkumaran, and Y. Matsushita, *ibid.* **177**, 3270 (2004); M. D. Smith and H. Loye, Chem. Mater. **12**, 2404 (2004); V. Eyert, U. Schwingenschlögl, R. Fresard, A. Maignan, C. Martin, N. Nguyen, C. Hackenberger, and T. Kopp, Phys. Rev. B **75**, 115105 (2007); S. Kawasaki and M. Takano, J. Solid State Chem. **145**, 302 (1999).
[11] K. E. Stitzer, J. Darriet, and H.-C. zur Loye, Curr. Opin. Solid State Mater. Sci. **5**, 535 (2001).
[12] J. B. Claridge, R. C. Layland, W. H. Henley, and H.-C. zur Loye, Chem. Mater. **11**, 1376 (1999).
[13] N. Mohapatra, K. K. Iyer, S. Rayaprol, and E. V. Sampathkumaran, Phys. Rev. B **75**, 214422 (2007).
[14] S. Majumdar, V. Hardy, M. R. Lees, D. McK. Paul, H. Rousseliere, and D. Grebille, Phys. Rev. B **69**, 024405 (2004).
[15] D. Flahaut, S. Hebert, A. Amignan, V. Hardy, C. Martin, M. Hervieu, M. Costes, B. Raquet, and J. M. Broto, Eur. Phys. J. B **35**, 317 (2003).
[16] T. N. Nguyen and H.-C. zur Loye, J. Solid State Chem. **117**, 300 (1995).
[17] O. K. Andersen, Phys. Rev. B **12**, 3060 (1975).
[18] O. K. Andersen and O. Jepsen, Phys. Rev. Lett. **53**, 2571 (1984).
[19] O. K. Andersen and T. Saha-Dasgupta, Phys. Rev. B **62**, R16219 (2000).
[20] G. Kresse and J. Hafner, Phys. Rev. B **47**, 558 (1993).
[21] G. Kresse and J. Furthmuller, Phys. Rev. B **54**, 11169 (1996).
[22] P. Blaha, K. Schwartz, G. K. H. Madsen, D. Kvasnicka, and J. Luitz, in *WIEN2K, An Augmented Plane Wave + Local Orbitals Program for Calculating Crystal Properties*, edited by K. Schwarz (Technische Universitat, Wien, Austria, 2001).
[23] S. K. Pandey and K. Maiti, EPL **88**, 27002 (2009).
[24] G. R. Zhang, X. L. Zhang, T. Jia, Z. Zeng, and H. Q. Lin, J. Appl. Phys. **107**, 09E120 (2010).
[25] A. P. Wilkinson, A. K. Cheetham, W. Kunnmann, and A. Kvick, Eur. J. Solid State Inorg. Chem. **28**, 453 (1991).
[26] J. P. Perdew, K. Burke, and M. Ernzerhof, Phys. Rev. Lett. **77**, 3865 (1996).
[27] C. J. Ballhausen, *Introduction to Ligand Field Theory* (McGraw-Hill, New York, 1962).
[28] T. N. Nguyen, D. M. Giaquinta, and H.-C. zur Loye, Chem. Mater. **6**, 1642 (1994).
[29] Note, the situation described for Sr_3NiIrO_6 compound is different from that obtained in Ref. 24. In Ref. 24, the $t_{2g}^{(3)}$ or a_{1g} level was found to be positioned lower than $t_{2g}^{(1)}$ and $t_{2g}^{(2)}$ or e_g^{π}'s. While the situation described in present work, leads to an insulating solution of Sr_3NiIrO_6 in spin-polarized calculations both within GGA and GGA+U, the authors in Ref. 24 needed to invoke the spin-orbit interaction to arrive to insulating state of Sr_3NiIrO_6.
[30] C. S. Helberg, W. E. Pickett, L. L. Boyer, H. T. Stokes, and M. J. Mehl, J. Phys. Soc. Jpn. **68**, 3489 (1999).
[31] V. I. Anisimov, I. V. Solovyev, M. A. Korotin, M. T. Czyzyk, and G. A. Sawatzky, Phys. Rev. B **48**, 16929 (1993).
[32] K. I. Kugel and D. I. Khomskii, Sov. Phys. Usp. **25**, 231 (1982).
[33] The values of the spin moments, particularly for Ir differ between Table III and the present one due to choice different sphere radii between LMTO basis and LAPW basis. A large part of the moment was found to be residing in the interstitial for LAPW calculation.
[34] C. Jia, S. Onoda, N. Nagaosa, and J. H. Han, Phys. Rev. B **76**, 144424 (2007).